19

Features of the formation of radiation spectra of two-particle nanosystems in a magnetic field

© M. G. Kucherenko, V. M. Nalbandyan, T. M. Chmereva

Center of Laser and Information Biophysics, Orenburg State University,
460018 Orenburg, Russia

e-mail: clibph@yandex.ru

Received November 13, 2021
Revised February 08, 2022
Accepted February 10, 2022

A spectral model of luminescence of the two-component exciton-activated semiconductor quantum dot (QD) layered plasmon composite nanoparticle (CNP) with a dielectric core and a conductive shell in an external magnetic field is constructed, taking into account the inhomogeneity of the quasi-stationary electric field generated by QD in the CNP region, outside the framework of the approximation of the dipole polarizability of the CNP. The tensor formalism of describing the characteristics of the field in each of the layers of the CNP, as well as outside the CNP, is used. It is established that with a change in the structure of the nanocomposite, the parameters of its core or shell layer, the spectral response of the system to external magnetic field action changes. It is shown that the special form of the response is associated with the characteristic magnetic properties of the nanoparticle components acquired (under the action of the field).

Keywords: plasma layered nanoparticle, spherical quantum dot, magnetic field, luminescence of a two-particle complex.

DOI: 10.21883/EOS.2022.05.54445.9-22

Introduction

Currently, hybrid nanostructures formed from single plasmonic and exciton nanoparticles (NP) are of great interest in connection with development of biosensors, ultrasensitive sensors and other nanophotonic devices, the principle of operation of which is based on the localization of the near electromagnetic field [1–5]. Exciton-plasmon interaction in such nanostructures makes it possible to control the processes of absorption and radiation, to control energy transfer from quantum dots (QDs) to composite NPs [6,7]. One of the important tasks of nanophotonics is to control the luminescence intensity of nanostructures formed from QDs, molecules, plasmonic NPs of various shapes, and also layered structures. Fundamental research in this area is important for understanding the features of the exciton-plasmon interaction and introducing new results into the industry of nanosystems [8–12].

Composite conductive NPs, in comparison with continuous homogeneous systems, make it possible to more flexibly control both the rates of intermolecular non-radiative transfer of electronic excitation energy [13] and the luminescence intensity of emitters [14–16]. In the article [15], the features of photoluminescence of quantum dipole emitters located near metal spherical NPs with a dielectric shell are theoretically considered. It is shown that in the case of a shelled NP, photoluminescence can be more intense than in the case of the same metal NP without a shell. In [16], an increase in emissivity of QDs near layered NPs with a dielectric shell was experimentally studied. The possibility of amplifying the QD radiation depending on NP shell thickness is demonstrated.

In articles [17–20], the real and imaginary parts of the dipole polarizability of single and cluster NPs in a quasi-homogeneous (on small scales) dipole field were studied. The possibility to control absorption and radiative processes in layered NPs by changing the electron-optical parameters of the system and the ratio of the radii of its core and shell is shown.

In some articles [21–23], the authors have shown that not only dipole but also multipole bands of higher orders are observed in the absorption spectra and scattering cross sections. In articles [24–26], it was experimentally found that the photoluminescence spectra of a two-component system of quantum emitters and metal NPs change in an external magnetic field. In the presence of magnetic field in such a system, a pronounced enhancement of luminescence was observed, while in the absence of plasmonic NPs, the effect of magnetic field enhancement of the luminescence was not observed.

In the present article, as well as in the article [11], the object of study was a two-particle cluster formed from an exciton-activated semiconductor QD and a two-layer plasmonic NP with the „core-shell“structure. However, in contrast to the article [11], where the consideration was carried out within the framework of the approximation of the dipole polarizability of a layered nanocomposite, in the present study, we went beyond the framework of the dipole approximation by taking into account multipole terms of a higher rank. A hybrid nanocomposite is considered, in

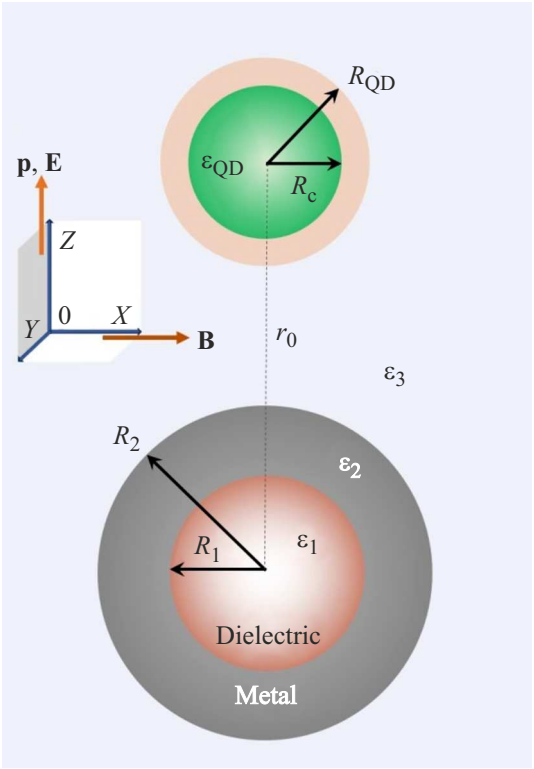

Figure 1. The geometrical configuration of the „layered NP−QD" system in magnetic field.

which the core and its conjugate shell form the „dielectric-metal" combination.

The two-particle system under study is an exciton-activated spherical semiconductor QD with radius R_{QD} (with an electron-hole pair or a Wannier-Mott exciton contained in it) and a globular layered metal-hybrid NP with radius R_2 with a core with radius R_1 located at a distance $r_0 > R_{QD} + R_2$ from QD (Fig. 1). The field $\mathbf{E}$ of a QD dipole source with electric dipole moment $\mathbf{p} = \mathbf{p}_0 \exp(-i\omega t)$ oscillates with frequency ω. In the simplest approximation of quasi-homogeneous field, it induces dipole moment $\mathbf{p}_2 = \varepsilon_3 \overleftrightarrow{\alpha}(\omega|\mathbf{B})\mathbf{E}$ in NP, where $\overleftrightarrow{\alpha}(\omega|\mathbf{B})$ — magnetically dependent dipole dynamic polarizability tensor of a composite nanoparticle (CNP). Precisely this simplified approach was implemented earlier in the articles [11,27]. In metal components of NPs placed in monochromatic field $\mathbf{E}(\omega)$, plasmon oscillations arise with a characteristic spectral composition determined by the radii of the shell and core, as well as by the dielectric permittivities $\varepsilon_1(\omega)$ and $\varepsilon_2(\omega)$.

The dielectric permittivity ε_{QD} of QDs was assumed to be constant in the frequency range of the exciton transition. The environment is assumed to be transparent at exciton frequencies and is characterized by a dielectric constant ε_3. Then, for a layered spherical NP, we will consider the case with a non-conducting core made of a material without dispersion, $\varepsilon_1 = \text{const}$. The shell is a conducting layer with strong frequency dispersion $\varepsilon_2(\omega)$.

In external magnetic induction field $\mathbf{B}$, the electron plasma of metal acquires anisotropic properties, and the dielectric permittivity of the conducting part of CNP becomes a tensor of the second rank $\varepsilon_2(\omega) \to \overleftrightarrow{\varepsilon}_2(\omega|\mathbf{B})$ [28]:

$$\overleftrightarrow{\varepsilon}_2(\omega|\mathbf{B}) = \begin{pmatrix} 1 - \frac{\omega_p^2}{\omega\kappa} & 0 & 0 \\ 0 & 1 - \frac{\omega_p^2\kappa}{\omega(\kappa^2 - \Omega_L^2)} & i\frac{\omega_p^2\Omega_L}{\omega(\kappa^2 - \Omega_L^2)} \\ 0 & -i\frac{\omega_p^2\Omega_L}{\omega(\kappa^2 - \Omega_L^2)} & 1 - \frac{\omega_p^2\kappa}{\omega(\kappa^2 - \Omega_L^2)} \end{pmatrix}, \quad (1)$$

where $\kappa = \omega + i\gamma$, γ — frequency of electron collisions (dissipation factor), $\omega_p = \sqrt{4\pi e^2 n_e/m^*}$ — Langmuir (plasma) frequency of metal electrons, $\Omega_L = eB/m^*c$ — Larmor (cyclotron) frequency of an electron with effective mass m^* in magnetic induction field B. The dielectric permittivity tensor $\overleftrightarrow{\varepsilon}(\omega|\mathbf{B})$ becomes (1) as the magnetic field induction vector $\mathbf{B}$ is directed along the X axis of the Cartesian coordinate system, and in the general case of an arbitrary orientation of the magnetic field induction vector, all nine components of this tensor are nonzero [28].

In the system under study, NP is located at the origin of coordinates, and QD is located at a distance r_0 from it along Z axis. Also, the dipole moment vector $\mathbf{p}$ of QD is directed parallel to the vector $\mathbf{r}_0$. To observe the effect of external magnetic field on the optical properties of a nanosystem, the condition must be satisfied under which the vector $\mathbf{B}$ is not parallel to the vectors $\mathbf{p}$ and $\mathbf{E}$. Therefore, the direction of the magnetic field vector along the X axis is selected.

Description of the QD electric field in the dipole approximation

In case of homogeneous spherical particles made of conducting material with dielectric permittivity $\varepsilon(\omega)$, their dipole dynamic polarizability $\alpha(\omega)$ in magnetic induction field $\mathbf{B}$ and in a non-dispersive dielectric medium with permittivity ε_3 takes the following tensor form [27]:

$$\overleftrightarrow{\alpha}(\omega|\mathbf{B}) = [\overleftrightarrow{\varepsilon}(\omega|\mathbf{B}) - \varepsilon_3 \overleftrightarrow{\mathbf{I}}][\overleftrightarrow{\varepsilon}(\omega|\mathbf{B}) + 2\varepsilon_3 \overleftrightarrow{\mathbf{I}}]^{-1}. \quad (2)$$

The dipole polarizability of a layered metal core composite is expressed as follows [29]:

$$\overleftrightarrow{\alpha}(\omega|\mathbf{B}) = \Big[(\overleftrightarrow{\varepsilon}_1(\omega|\mathbf{B}) + 2\varepsilon_2 \overleftrightarrow{\mathbf{I}})(\varepsilon_2 - \varepsilon_3) + (\overleftrightarrow{\varepsilon}_1(\omega|\mathbf{B}) - \varepsilon_2 \overleftrightarrow{\mathbf{I}})(2\varepsilon_2 + \varepsilon_3)\xi^3\Big]\Big[(\overleftrightarrow{\varepsilon}_1(\omega|\mathbf{B}) + 2\varepsilon_2 \overleftrightarrow{\mathbf{I}}) \times (\varepsilon_2 + 2\varepsilon_3) + 2(\overleftrightarrow{\varepsilon}_1(\omega|\mathbf{B}) - \varepsilon_2 \overleftrightarrow{\mathbf{I}})(\varepsilon_2 - \varepsilon_3)\xi^3\Big]^{-1} R_2^3, \quad (3)$$

where $\xi = R_1/R_2$, $\overleftrightarrow{\mathbf{I}}$ — the identity matrix with 3×3 dimension.

Dipole polarizability of composite with a magnetized conducting shell and a dielectric core [29] has the form

$$\begin{aligned}\overleftrightarrow{\boldsymbol{\alpha}}(\omega|\mathbf{B}) = &\Big[(\varepsilon_1\overleftrightarrow{\mathbf{I}} + 2\overleftrightarrow{\boldsymbol{\varepsilon}}_2(\omega|\mathbf{B}))(\overleftrightarrow{\boldsymbol{\varepsilon}}_2(\omega|\mathbf{B}) - \varepsilon_3\overleftrightarrow{\mathbf{I}})\\ &+ (\varepsilon_1\overleftrightarrow{\mathbf{I}} - \overleftrightarrow{\boldsymbol{\varepsilon}}_2(\omega|\mathbf{B}))(2\overleftrightarrow{\boldsymbol{\varepsilon}}_2(\omega|\mathbf{B}) + \varepsilon_3\overleftrightarrow{\mathbf{I}})\xi^3\Big]\\ &\times\Big[(\varepsilon_1\overleftrightarrow{\mathbf{I}} + 2\overleftrightarrow{\boldsymbol{\varepsilon}}_2(\omega|\mathbf{B}))(\overleftrightarrow{\boldsymbol{\varepsilon}}_2(\omega|\mathbf{B}) + 2\varepsilon_3\overleftrightarrow{\mathbf{I}})\\ &+ 2(\varepsilon_1\overleftrightarrow{\mathbf{I}} - \overleftrightarrow{\boldsymbol{\varepsilon}}_2(\omega|\mathbf{B}))(\overleftrightarrow{\boldsymbol{\varepsilon}}_2(\omega|\mathbf{B}) - \varepsilon_3\overleftrightarrow{\mathbf{I}})\xi^3\Big]^{-1}R_2^3. \qquad (4)\end{aligned}$$

The resonant frequencies of the imaginary part of the dipole polarizability of continuous and layered NPs differ from each other due to addition of an outer layer. In the dipole polarizability spectra of a layered particle with a metal (core)–dielectric (shell) structure, one characteristic spectral plasmon band appears, and in case of a reversed dielectric (core)–metal (shell) structure, two plasmonic spectral bands appear.

Heterogeneous quasi-stationary electric field of QD and polarized CNP

At small distances r_0 from QD or relatively large radii $R_2 \sim r_0$ of CNP, field $E(\omega)$ of the dipole $\mathbf{p}$ can no longer be considered homogeneous, and the method of electric dipole polarizability (2)–(4) often used to describe the response to homogeneous field becomes insufficiently correct. Below, we describe the model of magnetized anisotropic CNP polarized in an heterogeneous quasi-stationary electric field of exciton-activated QD.

Potentials $\varphi_j(r,\theta)$ $(j = 1, 2, 3)$ of the electric field inside the core $(j = 1,\ r < R_1)$, inside the shell $(j = 2,\ R_1 < r < R_2)$ and outside the composite $(j = 3,\ r > R_2)$ — in medium with dielectric permittivity ε_3 created by a point charge q placed at the point $(r_0, 0)$ $(r_0 > R_2)$ outside the layered ball, can be written as

$$\varphi_1(r,\theta;r_0|\mathbf{B}) = \sum_{l=0}^{\infty}\mathbf{r}_0\overleftrightarrow{\mathbf{D}}_l(\omega|\mathbf{B})\mathbf{r}_0\frac{r^l}{r_0^2R_1^l}P_l(\cos\theta),\ \ r < R_1, \qquad (5)$$

$$\varphi_2(r,\theta;r_0|\mathbf{B}) = \sum_{l=0}^{\infty}\Big[\mathbf{r}_0\overleftrightarrow{\mathbf{B}}_l(\omega|\mathbf{B})\mathbf{r}_0\frac{r^l}{r_0^2R_1^l} + \mathbf{r}_0\overleftrightarrow{\mathbf{C}}_l(\omega|\mathbf{B})\mathbf{r}_0\frac{R_2^{l+1}}{r_0^2r^{l+1}}\Big]P_l(\cos\theta),\ \ R_1 < r < R_2, \qquad (6)$$

$$\varphi_3(r,\theta;r_0|\mathbf{B}) = \frac{q}{\varepsilon_3R_{\mathrm{M}}} + \sum_{l=0}^{\infty}\mathbf{r}_0\overleftrightarrow{\mathbf{A}}_l(\omega|\mathbf{B})\mathbf{r}_0\frac{R_2^{l+1}}{r_0^2r^{l+1}}P_l(\cos\theta),\ \ r > R_2, \qquad (7)$$

where $P_l(\cos\theta)$ — the Legendre polynomial of degree l, θ — the angle defining the direction of the radius-vector $\mathbf{r}$ of the point where potential $\varphi_j(r,\theta)$ is calculated, $R_{\mathrm{M}} = |\mathbf{r} - \mathbf{r}_0|$ — distance between the center of the QD and the observation point M.

Tensors $\overleftrightarrow{\mathbf{A}}_l(\omega|\mathbf{B})$, $\overleftrightarrow{\mathbf{B}}_l(\omega|\mathbf{B})$, $\overleftrightarrow{\mathbf{C}}_l(\omega|\mathbf{B})$ and $\overleftrightarrow{\mathbf{D}}_l(\omega|\mathbf{B})$ can be found based on the boundary conditions on the interfaces of the NP layers, and the tensor $\overleftrightarrow{\mathbf{A}}_l(\omega|\mathbf{B})$, (up to a factor) is the 2^l-pole polarizability of spherical magnetized nanocomposite. All tensors $\overleftrightarrow{\mathbf{A}}_l$, $\overleftrightarrow{\mathbf{B}}_l$, $\overleftrightarrow{\mathbf{C}}_l$ and $\overleftrightarrow{\mathbf{D}}_l$ have dimension of the potential φ_j. We also take into account that

$$1/R_{\mathrm{M}} = \sum_{l=0}^{\infty}\frac{k^l}{r_0^{l+1}}P_l(\cos\theta),\quad r < r_0. \qquad (8)$$

Relations between unknown tensors $\overleftrightarrow{\mathbf{A}}_l$, $\overleftrightarrow{\mathbf{B}}_l$, $\overleftrightarrow{\mathbf{C}}_l$ and $\overleftrightarrow{\mathbf{D}}_l$ are found based on the conditions on the boundary spheres $S(R_1)$ and $S(R_2)$ taking into account (8):

$$\varphi_1(R_1,\theta) = \varphi_2(R_1,\theta),\ \ \varphi_2(R_2,\theta) = \varphi_3(R_2,\theta), \qquad (9)$$

$$\varepsilon_1\overleftrightarrow{\mathbf{I}}\left(\frac{\partial\varphi_1}{\partial r}\right)_{R_1} = \boldsymbol{\varepsilon}_2\left(\frac{\partial\varphi_2}{\partial r}\right)_{R_1},$$

$$\boldsymbol{\varepsilon}_2\left(\frac{\partial\varphi_2}{\partial r}\right)_{R_2} = \varepsilon_3\overleftrightarrow{\mathbf{I}}\left(\frac{\partial\varphi_3}{\partial r}\right)_{R_1}. \qquad (10)$$

Then from (5)–(7) and (9), (10) it follows

$$\overleftrightarrow{\mathbf{D}}_l = \overleftrightarrow{\mathbf{B}}_l + \overleftrightarrow{\mathbf{C}}_l\left(\frac{R_2}{R_1}\right)^{l+1},\quad \frac{qR_2^l}{\varepsilon_3r_0^{l+1}}\overleftrightarrow{\mathbf{I}} + \overleftrightarrow{\mathbf{A}}_l = \overleftrightarrow{\mathbf{B}}_l\left(\frac{R_2}{R_1}\right)^l + \overleftrightarrow{\mathbf{C}}_l, \qquad (11)$$

$$\varepsilon_1\overleftrightarrow{\mathbf{D}}_l = \overleftrightarrow{\boldsymbol{\varepsilon}}_2(\omega)\left[\overleftrightarrow{\mathbf{B}}_l - \overleftrightarrow{\mathbf{C}}_l\frac{(l+1)}{l}\left(\frac{R_2}{R_1}\right)^{l+1}\right], \qquad (12)$$

$$\frac{qR_2^{l-1}}{r_0^{l+1}}\overleftrightarrow{\mathbf{I}} - \varepsilon_3\overleftrightarrow{\mathbf{A}}_l\frac{(l+1)}{lR_2} = \overleftrightarrow{\boldsymbol{\varepsilon}}_2(\omega)\left[\overleftrightarrow{\mathbf{B}}_l\frac{R_2^{l-1}}{R_1^l} - \overleftrightarrow{\mathbf{C}}_l\frac{(l+1)}{lR_2}\right]. \qquad (13)$$

Sequentially eliminating tensors through linear transformations $\overleftrightarrow{\mathbf{A}}_l$, $\overleftrightarrow{\mathbf{C}}_l$ and $\overleftrightarrow{\mathbf{D}}_l$ from equations (11)–(13), for the tensor we obtain $\overleftrightarrow{\mathbf{B}}_l$ expression

$$\overleftrightarrow{\mathbf{B}}_l = \frac{q(2l+1)R_2^{l-1}}{r_0^{l+1}}\overleftrightarrow{\boldsymbol{\rho}}_l, \qquad (14)$$

where

$$\overleftrightarrow{\boldsymbol{\rho}}_l(\omega) = \left\{\overleftrightarrow{\boldsymbol{\eta}}_2^l(\omega|\mathbf{B})\frac{R_2^{l-1}}{R_1^l} + [\varepsilon_3\overleftrightarrow{\mathbf{I}} - \overleftrightarrow{\boldsymbol{\varepsilon}}_2(\omega)][\overleftrightarrow{\boldsymbol{\eta}}_1^l(\omega|\mathbf{B})]^{-1}\times[\overleftrightarrow{\boldsymbol{\varepsilon}}_2(\omega) - \varepsilon_1\overleftrightarrow{\mathbf{I}}]\frac{l(l+1)}{R_2}\left(\frac{R_1}{R_2}\right)^{l+1}\right\}^{-1},$$

$\overleftrightarrow{\boldsymbol{\eta}}_j^l(\omega|\mathbf{B}) = (l+1)\boldsymbol{\varepsilon}\overleftrightarrow{\boldsymbol{\eta}}_{j+1}(\omega|\mathbf{B}) + l\overleftrightarrow{\boldsymbol{\varepsilon}}_j(\omega|\mathbf{B})$, $\overleftrightarrow{\boldsymbol{\varepsilon}}_3 = \varepsilon_3\overleftrightarrow{\mathbf{I}}$, $\overleftrightarrow{\boldsymbol{\varepsilon}}_1 = \varepsilon_1\overleftrightarrow{\mathbf{I}}$, and tensor $[\overleftrightarrow{\boldsymbol{\eta}}_j^l(\omega|\mathbf{B})]^{-1}$ opposite to tensor $\overleftrightarrow{\boldsymbol{\eta}}_j^l(\omega|\mathbf{B})$. Tensor $\overleftrightarrow{\boldsymbol{\rho}}_l$ has length dimension.

For the tensor $\overleftrightarrow{\mathbf{C}}_l(\omega|\mathbf{B})$ we obtain

$$\overleftrightarrow{\mathbf{C}}_l(\omega|\mathbf{B}) = \frac{q(2l+1)lR_2^{l-1}}{r_0^{l+1}}\left(\frac{R_1}{R_2}\right)^{l+1} \times [\overleftrightarrow{\varepsilon}_2(\omega) - \varepsilon_1\overleftrightarrow{\mathbf{I}}][\overleftrightarrow{\boldsymbol{\eta}}_1^l(\omega|\mathbf{B})]^{-1}\overleftrightarrow{\boldsymbol{\rho}}_l. \quad (15)$$

The $\overleftrightarrow{\mathbf{D}}_l(\omega|\mathbf{B})$ tensor is defined by the first equation (11)

$$\overleftrightarrow{\mathbf{D}}_l(\omega|\mathbf{B}) = \frac{q(2l+1)R_2^{l-1}}{r_0^{l+1}} \times \left\{\overleftrightarrow{\mathbf{I}} + l[\overleftrightarrow{\varepsilon}_2(\omega) - \varepsilon_1\overleftrightarrow{\mathbf{I}}][\overleftrightarrow{\boldsymbol{\eta}}_1^l(\omega|\mathbf{B})]^{-1}\right\}\overleftrightarrow{\boldsymbol{\rho}}_l, \quad (16)$$

and for the $\overleftrightarrow{\mathbf{A}}_l$ tensor proportional to the 2^l-pole polarizability of layered composite with an anisotropic shell, the second equation (11) implies

$$\overleftrightarrow{\mathbf{A}}_l(\varepsilon_1, \overleftrightarrow{\varepsilon}_2, \varepsilon_3) = \frac{qR_2^l}{\varepsilon_3 r_0^{l+1}}\overleftrightarrow{\mathbf{I}} + \left[\xi^{-l}\overleftrightarrow{\mathbf{I}} + l\xi^{l+1}[\overleftrightarrow{\varepsilon}_2(\omega) - \varepsilon_1\overleftrightarrow{\mathbf{I}}] \times [\overleftrightarrow{\boldsymbol{\eta}}_1^l(\omega|\mathbf{B})]^{-1}\right]\frac{q(2l+1)R_2^{l-1}}{r_0^{l+1}}\overleftrightarrow{\boldsymbol{\rho}}_l. \quad (17)$$

When the magnetic field is turned off, all tensor quantities are reduced to scalars, so the tensors (14)–(17) are transformed to the previously obtained scalar expressions for isotropic composite.

Potentials $\delta\varphi_j(r, \theta|\mathbf{B})$, $(j = 1, 2, 3)$ of the NP near electric field initiated by a radially aligned $\mathbf{p}_0 = q\delta\mathbf{r}_0$ point dipole, we obtain by differentiating the potentials $\varphi_j(r, \theta)$ given by the expressions (5)–(7), by variable r_0: $\delta\varphi_j(r, \theta) = \nabla(r_0)\varphi_j(r, \theta)|r_)\delta r_0$,

$$\delta\varphi_1(r,\theta;r_0|\mathbf{B}) = -\sum_{l=0}^{\infty}\mathbf{p}_0\left[\overleftrightarrow{\mathbf{I}} + l[\overleftrightarrow{\varepsilon}_2(\omega) - \varepsilon_1\overleftrightarrow{\mathbf{I}}] \times [\overleftrightarrow{\boldsymbol{\eta}}_1^l(\omega|\mathbf{B})]^{-1}\right]\overleftrightarrow{\boldsymbol{\rho}}_l\mathbf{r}_0\frac{(2l+1)(l+1)R_2^{l-1}r^l}{r_0^{l+3}R_1^l} \times P_l(\cos\theta),\ r < R_1, \quad (18)$$

$$\delta\varphi_2(r, \theta; r_0|\mathbf{B}) = -\sum_{l=0}^{\infty}\frac{(2l+1)(l+1)R_2^{l-1}}{r_0^{l+3}} \times \mathbf{p}_0\left[\frac{r^l}{R_1^l}\overleftrightarrow{\mathbf{I}} + [\overleftrightarrow{\varepsilon}_2(\omega) - \varepsilon_1\overleftrightarrow{\mathbf{I}}][\overleftrightarrow{\boldsymbol{\eta}}_1^l(\omega|\mathbf{B})]^{-1}l\frac{R^{l+1}}{r^{l+1}}\right] \times \overleftrightarrow{\boldsymbol{\rho}}_l\mathbf{r}_0P_l(\cos\theta),\ R_1 < r < R_2, \quad (19)$$

$$\delta\varphi_3(r, \theta; r_0|\mathbf{B}) = \frac{p_0}{\varepsilon_3 R_{\mathrm{M}}^3}(r\cos\theta - r_0) - \sum_{l=0}^{\infty}\mathbf{p}_0\frac{(l+1)}{r^{l+1}} \times P_1(\cos\theta)\left\{-\frac{R_2^{2l+1}}{\varepsilon_3 r_0^{l+3}}\overleftrightarrow{\mathbf{I}} + \left[\xi^{-l}\overleftrightarrow{\mathbf{I}} + \xi^{l+1}[\overleftrightarrow{\varepsilon}_2(\omega) - \varepsilon_1\overleftrightarrow{\mathbf{I}}] \times [\overleftrightarrow{\boldsymbol{\eta}}_1^l(\omega|\mathbf{B})]^{-1}\right]\frac{(2l+1)lR_2^{2l}}{r_0^{l+3}}\overleftrightarrow{\boldsymbol{\rho}}_l\right\}\mathbf{r}_0,\ r > R_2. \quad (20)$$

The quasi-stationary field (20) with the potential $\delta\varphi_3(r, \theta; r_0|\mathbf{B})$ determines the non-radiative energy transfer from the exciton-activated QD near the conducting NP to the molecule, a molecular cluster, or a small acceptor particle with radius r_{M} in magnetic field. The speed w_{DA} of such a process is proportional to the square of the scalar product of vectors, $w_{\mathrm{DA}} \sim \left(\mathbf{p}_{\mathrm{A}}\nabla\delta\varphi_3(r, \theta; r_0|\mathbf{B})\right)^2$ [27].

Luminescence of binary „layered plasmonic NP–QD“ complexes in magnetic field

Identified with the luminescence signal, the spectral density N of the number of photons emitted by the combined „QD–layered NP“ system at frequency ω has the form [11,12]

$$N(\omega|\mathbf{B}, r_0) = \frac{1}{2\pi}\frac{w_{sp}^2(\omega|\mathbf{B}, r_0)\Gamma(\omega|\mathbf{B}, r_0)}{(\omega - \omega_{ij})^2 + \Gamma^2(\omega|\mathbf{B}, r_0)}, \quad (21)$$

where the function of the spectral width of the Lorentz luminescence line $\Gamma(\omega|\mathbf{B}, r_0) = w_{sp}(\omega|\mathbf{B}, r_0) + U(\omega|\mathbf{B}, r_0) + K$.

When the CNP dipole moment $\mathbf{p}_2$ is formed in the heterogeneous field of QD, the formula for the rate $w_{sp}(\omega|\mathbf{B}, \mathbf{r})$ of spontaneous radiation by a combined binary „QD–layered NP“ system can be written in the following form:

$$w_{sp}(\omega|\mathbf{B}, r_0) = = \frac{4}{3}\frac{\omega^3}{\hbar c^3}\left|\mathbf{p}_2(r_0|\mathbf{B}) + \frac{3\varepsilon_3}{\varepsilon_1 + 2\varepsilon_3}\int_0^{R_c}\mathbf{P}(r)4\pi r^2dr\right|^2. \quad (22)$$

The polarization vector $\mathbf{P}(r)$ of an activated QD in the regime of strong confinement of an electron and a hole is defined by the expression [11,12]

$$\mathbf{P}(\mathbf{r}) = \frac{\mathbf{p}_0}{2\pi R_c}\frac{\sin^2(\pi r/R_c)}{r^2},$$

where $\mathbf{p}_0$ — the vector matrix element of the interband electronic dipole transition moment, r – the distance from the QD center to the localization point of the $e-h$-pair $(r = r_e = r_h)$.

The integral $\mathbf{p}_2(r_0|\mathbf{B})$ in (22) is the induced CNP dipole moment in the heterogeneous field of the activated QD and

in the induction magnetic field **B**:

$$\mathbf{p}_2(r_0|\mathbf{B}) = -\frac{1}{2}[\overleftrightarrow{\varepsilon}_2(\omega)]^{-1} \times \int_0^{R_1}\int_0^{\pi}[\varepsilon_1 \overleftrightarrow{\mathbf{I}} - \overleftrightarrow{\varepsilon}_2(\omega)]\nabla_{\mathbf{r}}\delta\varphi_1(r,\theta|\mathbf{B})r^2 dr\sin\theta d\theta - \frac{1}{2\varepsilon_3}\int_{R_1}^{R_2}\int_0^{\pi}[\overleftrightarrow{\varepsilon}_2(\omega) - \varepsilon_3\overleftrightarrow{\mathbf{I}}]\nabla_{\mathbf{r}}\delta\varphi_2(r,\theta|\mathbf{B})r^2 dr\sin\theta d\theta. \quad (23)$$

To calculate the induced dipole moment in a layered composite particle, it is necessary to determine the potential gradients (18) and (19) in the core and shell of the nanocomposite. The potential gradient (20) will determine the rate of non-radiative transfer of electronic excitation energy from the layered NP to the acceptor particle, if it is in the near region of the QD and CNP.

It is easy to show that both integrals in (23) contain only dipole-type contributions from the multipole series (18) and (19). Indeed, by calculating the gradient from the potential (18), we obtain the expressions

$$\nabla_{\mathbf{r}}[r^l P_l(\cos\theta)] = \sqrt{4\pi l}\, r^{l-1}\mathbf{Y}_{l0}^{l-1}(\theta),$$

where $\mathbf{Y}_{lm}^{l}(\theta,\varphi)$ — a spherical vector [30]. Considering that the integral of the spherical vector $\mathbf{Y}_{lm}^{l}(\theta,\varphi)$ over the solid angle is equal to

$$\int \mathbf{Y}_{JM}^{L}(\theta,\varphi)d\Omega = \sqrt{4\pi}\delta_{J1}\delta_{l0}\mathbf{e}_M,$$

we come to the conclusion that only the dipole term with $l = 1$ from the sum (18) makes a nonzero contribution to the integral (23). We arrive at a similar result when calculating the gradient from the potential (19). For the second part (19) we obtain

$$\nabla_{\mathbf{r}}[r^{-(l+1)}P_l(\cos\theta)] = \sqrt{4\pi(l+1)}\, r^{-(l+2)}\mathbf{Y}_{l0}^{l+1}(\theta),$$

whence it follows that the integrals of this part are equal to zero for all indices l.

The rate $U(\omega|\mathbf{B}, r_0)$ of non-radiative energy transfer from QD to CNP in case of heterogeneous QD field can be represented by the sum of two integrals of the imaginary parts of the quadratic forms of the local field intensity vectors $-\nabla_{\mathbf{r}}\delta\varphi_{1,2}(r,\theta|\mathbf{B}) = \mathbf{E}_{1,2}(r,\theta|\omega)$ inside the layered NP:

$$U(\omega|\mathbf{B}, r_0) = \frac{1}{2\pi\hbar} \times \int_0^{R_1}\int_0^{\pi}\mathrm{Im}\mathbf{E}_1^*(r,\theta|\omega)\varepsilon_1\mathbf{E}_1(r,\theta|\omega)\sin\theta d\theta r^2 dr + \frac{1}{2\pi\hbar}\int_{R_1}^{R_2}\int_0^{\pi}\mathrm{Im}\mathbf{E}_2^*(r,\theta|\omega)\overleftrightarrow{\varepsilon}_2(\omega)\mathbf{E}_2(r,\theta|\omega)\sin\theta d\theta r^2 dr. \quad (24)$$

Now the integrals in (24) for the rate $U(\omega|\mathbf{B}, r_0)$ contain the quadratic form of the potential gradient, which means that the nonzero contribution to the total rate $U(\omega|\mathbf{B}, r_0)$ will now also be made by higher terms of the series of potentials (18) and (19).

In case of an isotropic core (scalar dielectric constant ε_1) in the first integral (24) for the subintegral function we obtain $|\mathbf{E}(r,\theta|\omega)|^2$, and the double sum over the indices l and l' of the integrals for this quantity, taking into account the orthonormality relation for spherical vectors,

$$\int \mathbf{Y}_{JM}^{L'*}(\theta,\varphi)\mathbf{Y}_{JM}^{L}(\theta,\varphi)d\Omega = \delta_{J'J}\delta_{L'L}\delta_{M'M}$$

turns into a sum over only one index l of the integral terms of the form

$$\int_0^{R_1} r^{2(l-1)}r^2 dr = \frac{1}{2l+1}R_1^{2l+1},$$

i.e. now the contribution from all higher terms of the series to the first integral (24) is nonzero. We come to a similar conclusion when calculating the second integral in (24).

In case of zero imaginary part ($\mathrm{Im}\varepsilon_1 = 0$) of the dielectric permittivity of the dissipativeless material of the CNP core, the first integral in (24) does not contribute to the general expression for the energy transfer rate. Then, the irreversible non-radiative energy transfer from QD is directed exclusively to the CNP shell (the second integral (24)).

Discussion of results

When calculating the rate spectra of radiative and non-radiative processes, the following values of the system parameters were used: $\omega_p = 13.87\cdot 10^{15}\,\mathrm{s}^{-1}$, $\gamma = 1.6\cdot 10^{14}\,\mathrm{s}^{-1}$, $B = 0\,\mathrm{T}$, $R_1 = 5\,\mathrm{nm}$, $R_2 = 8\,\mathrm{nm}$, $R_c = 4\,\mathrm{nm}$, $R_{\mathrm{QD}} = 5\,\mathrm{nm}$, $r_{\mathrm{B}} = 5\,\mathrm{nm}$, $r_0 = R_2 + R_{\mathrm{QD}} + 2\,\mathrm{nm}$, $p_0 = 12\,\mathrm{D}$, $\varphi_1 = 1.2$, $\varphi_3 = 2$, $\varphi_{\mathrm{QD}} = 6$, $\omega_{if} = 6.3\cdot 10^{15}\,\mathrm{s}^{-1}$, $K = 10^{14}\,\mathrm{s}^{-1}$.

The values of the quantities that changed in the course of the calculations are additionally indicated in the captions to the figures. The values of quantities typical for QDs are taken from [31]. As NPs with pronounced plasmonic properties, the authors of many experimental works often use single-component or composite gold NPs. For this reason, in the present article, the values of parameters typical for such metals as Au or Ag were selected for calculations.

The rate of non-radiative energy transfer from QD to CNP. The contribution of terms of different orders for the potentials of the electric field inside NP was taken into account by summing over the index l of a finite number n of the first terms of the series ($\sum_{l=0}^{\infty} \to \sum_{l=0}^{n}$) in formulas (18) and (19).

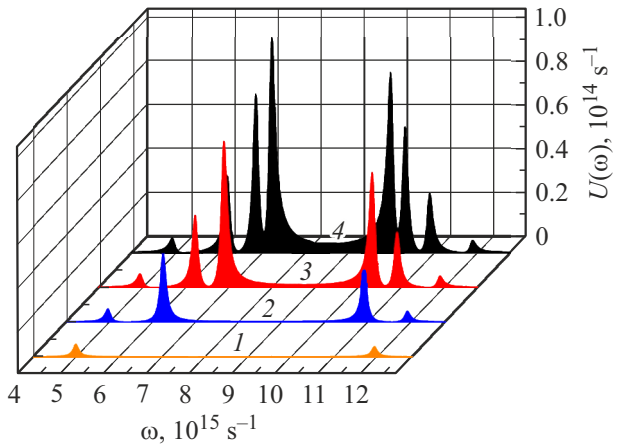

Figure 2. Rate spectra of non-radiative energy transfer from QD to layered NP at different values n: *1* — 1, *2* — 2, *3* — 3, *4* — 4. $R_1 = 5$, $\Delta_{NP} = 3$ nm.

Figure 2 (for $n = 1$) shows two spectral bands that differ from each other in amplitude and are located at frequencies $\omega_1 = 5 \cdot 10^{15}\ s^{-1}$ and $\omega_2 = 1.2 \cdot 10^{16}\ s^{-1}$. For a system with NPs, consisting of a dielectric core and a metal shell with thickness $\Delta_{NP} = R_2 - R_1$, two spectral bands are observed associated with the presence of two characteristic plasmonic resonances, in contrast to a system with NPs of a metal core and a dielectric shell, where only one spectral band is observed. Appearance of an additional spectral band is explained by the presence of two metal-dielectric interfaces: the metal shell – the dielectric core and the metal shell – the environment.

It follows from Fig. 2 ($R_1 > \Delta_{NP}$) that as the integer number n increases, new spectral bands appear, the amplitude of which is larger than the previous ones, and for $R_1 < \Delta_{NP}$ (Fig. 3) with an increase in n, the amplitude of such bands, on the contrary, decreases. So, for $n = 1$ two spectral bands are observed, $n = 2$ — four bands, $n = 3$ — six, $n = 4$ — eight bands.

Rate of spontaneous radiation of the „layered NP−QD“system. The rate of spontaneous radiation of the combined binary „layered NP−QD“ system was calculated by formula (22).

Figure 4 shows the rate spectra of spontaneous emission of a two-particle system with an increase in the thickness of the CNP metal layer: in the low-frequency region, the amplitudes of the spectral peaks increase, while in the high-frequency region, they decrease. This shifts the resonant frequencies of both peaks.

As the distance r_0 between two particles increases, the rate of spontaneous emission decreases. The opposite situation is observed with an increase in the dipole moment of the interband transition p_0 in QD.

Luminescence of the „layered NP−QD“system. The spectral density of the number of photons (luminescence intensity) emitted by the combined binary „layered NP−QD“ system was calculated by formula (21).

With an increase in the core radius R_1 of a layered NP at constant thickness Δ_{NP} of the shell, the amplitude of the high-frequency spectral band increases in the luminescence spectrum of the system (Fig. 5). In the low-frequency region of the spectrum, a comparatively sharp decrease in the amplitude of the characteristic spectral band occurs. In this case, the spectral bands in the low- and high-frequency regions are shifted in opposite directions.

In case of small core radius and sufficiently large shell thickness, the parameter $\xi \ll 1$, and then the only noticeable, high-amplitude plasmon resonance of the composite polarizability occurs at frequency ω_{res}:

$$\omega_{res} = \frac{\omega_p}{\sqrt{\varepsilon_\infty + 2\varepsilon_3}}\left[1 - \frac{1}{8}\frac{\gamma^2}{\omega_p^2}(\varepsilon_\infty + 2\varepsilon_3)\right], \qquad (25)$$

i.e. as in the case of a homogeneous metal sphere with dielectric permittivity $\varepsilon_2(\omega)$. When writing (25), we took into account that $\gamma^2/\omega_p^2 \ll 1$. In the more general case of an arbitrary value of the parameter $\xi \leq 1$, the plasmon resonance in the absorption (scattering) of light, as well as in the considered case of the luminescence of a two-particle system, will be observed when the following tensor from formula (4) tends to zero:

$$\left[(\varepsilon_1 \overleftrightarrow{\mathbf{I}} + 2\overleftrightarrow{\varepsilon}_2(\omega|\mathbf{B}))(\overleftrightarrow{\varepsilon}_2(\omega|\mathbf{B}) + 2\varepsilon_3 \overleftrightarrow{\mathbf{I}}) + 2(\varepsilon_1 \overleftrightarrow{\mathbf{I}} - \overleftrightarrow{\varepsilon}_2(\omega|\mathbf{B}))(\overleftrightarrow{\varepsilon}_2(\omega|\mathbf{B}) - \varepsilon_3 \overleftrightarrow{\mathbf{I}})\xi^3\right] \to 0. \qquad (26)$$

Further considering for simplicity the scalar version of the problem (i.e. in the absence of magnetic field) for two zeros of the function (26), in this case we obtain

$$\varepsilon_2^{\pm}(\omega_{res}) = -\beta \pm \sqrt{\beta^2 - \varepsilon_1\varepsilon_3}, \qquad (27)$$

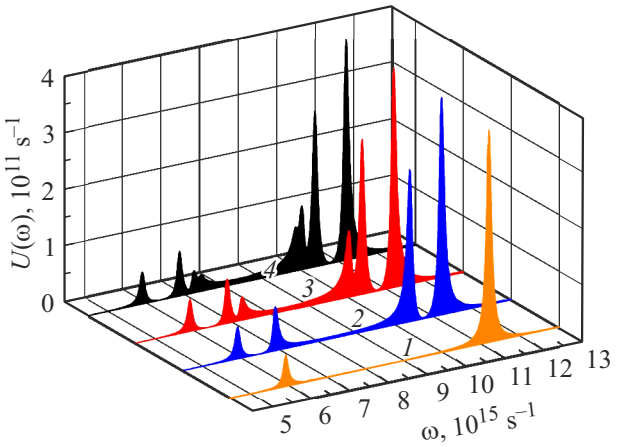

Figure 3. Rate spectra of non-radiative energy transfer from QD to layered NP at different values n: *1* — 1, *2* — 2, *3* — 3, *4* — 4. $R_1 = 3$, $\Delta_{NP} = 5$ nm.

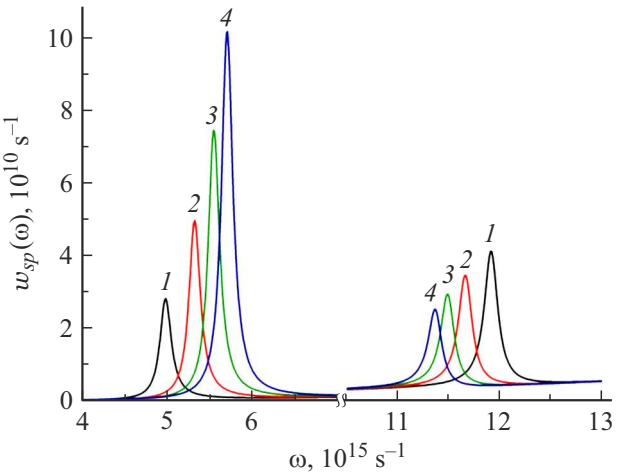

Figure 4. Rate spectra of spontaneous emission of the „QD−CNP" complex depending on the thickness Δ_{NP} of the CNP metal shell. Values for Δ_{NP}: *1* — 3, *2* — 4, *3* — 5, *4* — 6 nm.

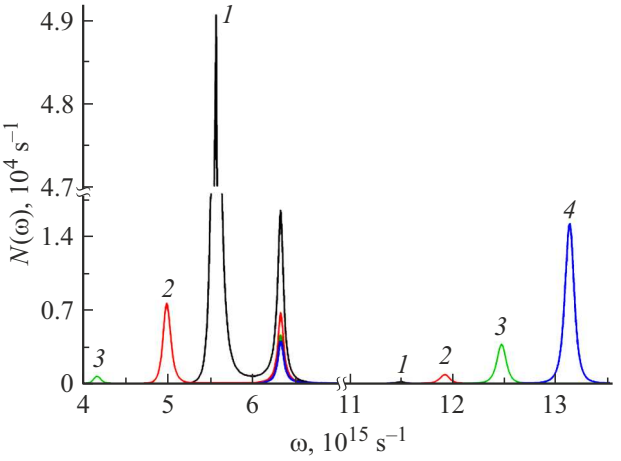

Figure 5. Luminescence spectra of the „layered NP−QD" system depending on the radius of the dielectric core R_1. Values R_1: *1* — 4, *2* — 5, *3* — 6, *4* — 7 nm.

where

$$\beta = \frac{[(\varepsilon_1 + 4\varepsilon_3) + 2\xi^3(\varepsilon_1 + \varepsilon_3)]}{4(1-\xi^3)}. \qquad (28)$$

From equation (27) we obtain two resonant frequencies $\omega_{res}^{\pm}$ for collective electron oscillations of the shell. They can be obtained in a simple way, as, for example, in [32]:

$$\omega_{res}^{\pm} = \frac{\omega_p}{\sqrt{\varepsilon_\infty + \beta_0 \pm \sqrt{\beta_0^2 - \varepsilon_1\varepsilon_3}}} \times \left[1 - \frac{1}{8}\frac{\gamma^2}{\omega_p^2}\left(\varepsilon_\infty + \beta_0 \pm \sqrt{\beta_0^2 - \varepsilon_1\varepsilon_3}\right)\right]. \qquad (29)$$

Here in (29) the zero approximation value β_0 is defined by expression (28) for $\varepsilon_1 \approx$ const.

In the particular case of hollow nanocomposite consisting of only one plasmonic shell ($\varepsilon_1 = \varepsilon_3 = \varepsilon_\infty = 1$) in air (vacuum), the formula (27) goes into

$$\varepsilon_2^{\pm}(\omega_{res}) = -\frac{5 + 4\xi^3}{4(1-\xi^3)} \pm \frac{3\sqrt{(1+8\xi^3)}}{4(1-\xi^3)}, \qquad (27')$$

and formula (29), neglecting the plasmon attenuation constant $\gamma \ll \omega_p$ — into the formula

$$\omega_{res}^{\pm} = \frac{\omega_p}{\sqrt{2}}\left[1 \pm \frac{\sqrt{(1+8\xi^3)}}{3}\right]. \qquad (29')$$

It is in the form (27′) and (29′) that the quantities are given, for example, in the article [33]. „Scattering" of resonant frequencies of shell spherical NPs with increasing core radius is a well-known result in nanoplasmonics, which directly follows from formulas (29) and (29′).

A change in the dielectric permittivity ε_1 of the non-conducting core of composite affects the luminescence spectrum of the system differently. Thus, with an increase in ε_1, the luminescence intensity increases in the high-frequency region, but decreases in the low-frequency region (Fig. 6, *a*). And an increase in the dielectric permittivity of the environment ε_3 leads to a gradual decrease in the radiation rate at all frequencies (Fig. 6, *b*). Both plots show a shift of the spectral bands to the low-frequency region.

Figure 7 shows the influence of the magnetic field on the luminescence of the „layered NP−QD" system. As the frequency γ of shell metal electron collisions decreases by three orders of magnitude, the luminescence intensity of the complex of CNPs with a metal shell increases by 12 orders of magnitude, in connection with this, the conditionally exciton band at the frequency $\omega_{if} = 6.3 \cdot 10^{15}$ s^{-1} becomes invisible due to the incommensurability in amplitude with two plasmonic bands, which experience splitting into two characteristic components in magnetic field. Spectral luminescence curves are deformed in magnetic field, first decreasing in amplitude and then splitting into two components, the distance between which increases with increasing magnetic field intensity. Figure 8 shows the luminescence spectrum of an inverted system consisting of NPs with a metal core and a dielectric shell. The difference between this CNP and composites with a conducting shell is that, with such a sequence of NP layers, only one spectral band is observed in its luminescence spectrum.

Conclusion

Based on the developed theoretical model, the rates of non-radiative energy transfer from QDs to layered NPs with a conducting shell, spontaneous radiation rates, and luminescence spectra of two-particle systems consisting of layered NPs and QDs placed in constant magnetic field were calculated. It is found that of all the components of the multipole series for the field in CNP, only dipole-type terms contribute to the radiation spectra of the considered systems, while the higher terms of the multipole series for the field potentials in the core and shell of CNP will also

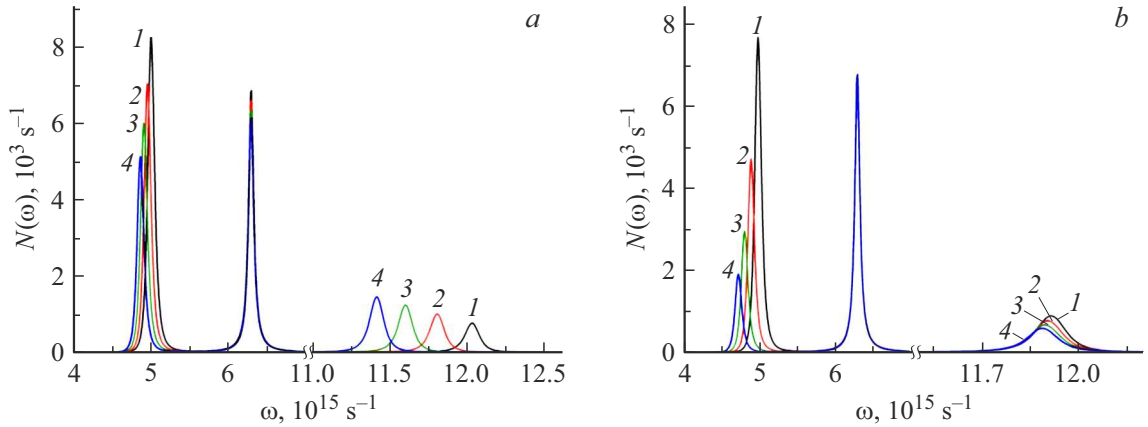

Figure 6. Luminescence spectra of the „layered NP−QD“ system depending on the dielectric permittivity of the core ε_1 (*a*) and the environment ε_3 (*b*). Values ε_1: *1* — 1.1, *2* — 1.3, *3* — 1.5, *4* — 1.7. Values ε_3: *1* — 2, *2* — 2.1, *3* — 2.2, *4* — 2.3.

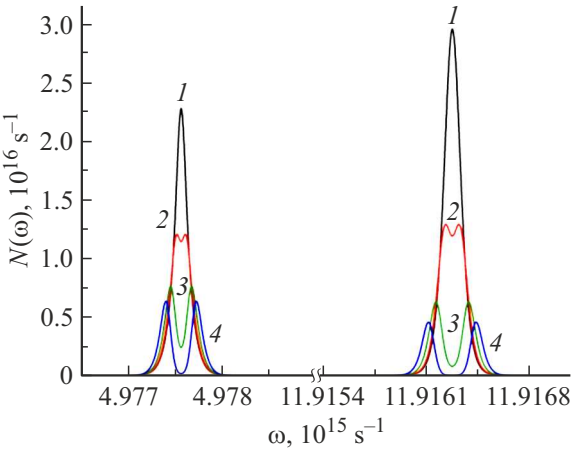

Figure 7. Luminescence spectra of the „layered NP (metal/dielectric)−QD“ system depending on the induction B of the external magnetic field. $\gamma = 1.6 \cdot 10^{11}\,\mathrm{s}^{-1}$. Values B: *1* — 0, *2* — 1, *3* — 2, *4* — 3 t.

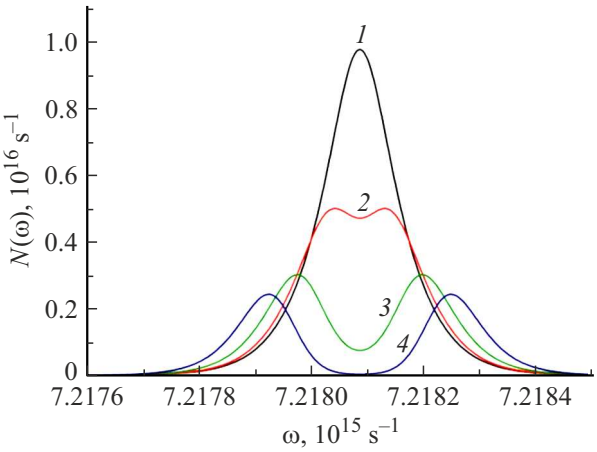

Figure 8. Luminescence spectra of the inverted „layered NP (metal/dielectric)−QD“ system depending on the induction B of the external magnetic field. $\gamma = 1.6 \cdot 10^{11}\,\mathrm{s}^{-1}$. Values B: *1* — 0, *2* — 1, *3* — 2, *4* — 3 t.

make a nonzero contribution to the rate of non-radiative energy transfer from QD to NCP. In this connection, in the rate spectra of non-radiative energy transfer, an increase in the number of spectral bands is observed with an increase in the number of terms of the series taken into account for the field potential in CNP.

It has been established that when induction of the external magnetic field changes, the radiative and non-radiative spectra of the energy transfer rate and luminescence spectra are transformed, the plasmon bands of which decrease in amplitude and split into two spectral components, the distance between which increases with increasing magnetic field induction.

The results obtained provide additional information for understanding the features of the exciton-plasmon interaction in magnetized nanosystems and can be used in the formation of the industry of metal-hybrid nanosystems, in development of non-contact optical sensors and devices for measuring the characteristics of constant magnetic field.

Funding

The study was supported financially by the Ministry of Science and Higher Education of the Russian Federation within the scope of the scientific project № FSGU-2020-0003.

Conflict of interest

The authors declare that they have no conflict of interest.

References

[1] V.I. Balykin, P.N. Melentiev. Phys. Usp., **61**, 133 (2018). DOI: 10.3367/UFNe.2017.06.038163

[2] S.I. Lepeshov, A.E. Krasnok, P.A. Belov, A.E. Miroshnichenko. Phys. Usp., **61**, 1035 (2018). DOI: 10.3367/UFNe.2017.12.038275
[3] E. Cao, Lin W., M. Sun, W. Liang, Y. Song. Nanophotonics, **7** (1), 145 (2018). DOI: 10.1515/nanoph-2017-0059
[4] A.P. Litvin, I.V. Martynenko, F. Purcell-Milton, A.V. Baranov, A.V. Fedorov, Y.K. Gun'ko. J. Mater. Chem. A, **5** (26), 13252 (2017). DOI: 10.1039/C7TA02076G
[5] S. Yan, X. Zhu, J. Dong, Y. Ding, S. Xiao. Nanophotonics, **9** (7), 1877 (2020). DOI: 10.1515/nanoph-2020-0074
[6] M. Achermann. J. Phys. Chem. Lett., **1**, 2837. DOI: 10.1021/JZ101102E
[7] E. Cohen-Hoshen, G.W. Bryant, I. Pinkas, J. Sperling, I. Bar-Joseph. Nano Letters, **12** (8), 4260 (2012). DOI: 10.1021/nl301917d
[8] J. Sun, H. Hu, D. Zheng, D. Zhang, Q. Deng, S. Zhang, H. Xu. ACS Nano, **12** (10), 10393 (2018). DOI: 10.1021/acsnano.8b05880
[9] T.J. Antosiewicz, S.P. Apell, T. Shegai. ACS Photonics, **1** (5), 454 (2014). DOI: 10.1021/ph500032d
[10] O. Bitton, S.N. Gupta, G. Haran. Nanophotonics, **8** (4), 559 (2019). DOI: 10.1515/nanoph-2018-0218
[11] M.G. Kucherenko, V.M. Nalbandyan, T.M. Chmereva. J. Opt. Technol., **88** (9), 489 (2021). DOI: 10.1364/JOT.88.000489
[12] M.G. Kucherenko, V.M. Nalbandyan. Opt. Spectrosc., **128** (11), 1910 (2020). DOI: 10.1134/S0030400X20110156.
[13] P. Rajput, M.S. Shishodia Plasmonics., **15** (6), 2081 (2020). DOI: 10.1007/s11468-020-01208-5
[14] H. Yanagawa, A. Inoue, H. Sugimoto, M. Shioi, M. Fujii. J. Appl. Phys., **122**, 223101 (2017). DOI: 10.1063/1.5001106
[15] D.V. Guzatov, S.V. Gaponenko. Doklady Nats. akad. nauk Belarusi, **63** (6), 689 (2020) (in Russian). DOI: 10.29235/1561-8323-2019-63-6-689-694
[16] A.K. Tobias, M. Jones. The J. Phys. Chem. C, **123** (2), 1389 (2018). DOI: 10.1021/acs.jpcc.8b09108
[17] M.G. Kucherenko, V.M. Nalbandyan. Vestnik OGU, **188** (13), 156 (2015) (in Russian).
[18] M.G. Kucherenko, V.M. Nalbandyan. Russian Physics J., **59** (9), 1425 (2017). DOI: 10.1007/s11182-017-0926-9.
[19] A.V. Korotun, A.A. Koval. Opt. i spektr., **127** (12), 1032 (2019) (in Russian). DOI: 10.21883/OS.2019.12.48705.133-19
[20] A.V. Korotun, V.V. Pogosov. FTT, **63** (1), 120 (2021) (in Russian). DOI: 10.21883/FTT.2021.01.50409.178
[21] P. Li, K. Du, F. Lu, K. Gao, F. Xiao, W. Zhang, T. Mei. J. Phys. Chem. C, **124** (35), 19252 (2020). DOI: 10.1021/acs.jpcc.0c05661
[22] I.Y. Goliney, V.I. Sugakov, L. Valkunas, G.V. Vertsimakha. Chem. Phys., **404**, 116 (2012). DOI: 10.1016/j.chemphys.2012.03.011
[23] K. Sakai, K. Nomura, T. Yamamoto, K. Sasaki. Scientific Reports, **5** (1), 1 (2015). DOI: 10.1038/srep08431
[24] Z.W. Ma, J.P. Zhang, X. Wang, Y. Yu, J.B. Han, G.H. Du, L. Li. Optics Letter, **38** (19), 3754 (2013). DOI: 10.1364/OL.38.003754
[25] C.M. Briskina, A.P. Tarasov, V.M. Markushev, M.A. Shiryaev. J. Nanophotonics. **12** (4), 043506 (2018). DOI: 10.1117/1.JNP.12.043506.
[26] Ch.M. Briskina, A.P. Tarasov, V.M. Markushev, M.A. Shiryaev. Zhurn. priklad. spektrosk., **85** (6), 1018 (2018) (in Russian).
[27] M.G. Kucherenko, V.M. Nalbandyan. Physics Procedia, **73**, 136 (2015). DOI: 10.1016/j.phpro.2015.09.134
[28] V.L. Ginzburg, A.A. Rukhadze. *Volny v magnitoaktivnoy plazme* (Nauka, M., 1975) (in Russian).
[29] M.G. Kucherenko, V.M. Nalbandyan. J. Opt. Technol., **85** (9), 524 (2018). DOI: 10.1364/JOT.85.000524
[30] D.A. Varshalovich, B.K. Khersonskiy, E.V. Orlenko, A.N. Moskalev. *Kvantovaya teoriya uglovogo momenta i ee prilozheniya*. V. 1 (Fizmatlit, M., 2017) (in Russian).
[31] V.M. Agranovich, D.M. Basko. Pis'ma v ZhETF, **69** (3), 232 (1999) (in Russian).
[32] M.G. Kucherenko, I.R. Alimbekov, P.P. Neyasov. Khim. fizika i mezoskopiya, **23** (3), 272 (2021) (in Russian). DOI: 10.15350/17270529.2021.3.25
[33] V.V. Klimov. *Nanoplazmonika* (Fizmatlit, M., 2009) (in Russian).